Is there a signal of sea-level rise in Chesapeake Bay salinity?

T. W. Hilton,[1] R. G. Najjar,[1] L. Zhong,[2] and M. Li[2]

Received 28 March 2007; revised 21 April 2008; accepted 22 May 2008; published 3 September 2008.

[1] We evaluate the hypothesis that sea-level rise over the second half of the 20th century has led to detectable increases in Chesapeake Bay salinity. We exploit a simple, statistical model that predicts monthly mean salinity as a function of Susquehanna River flow in 23 segments of the main stem Chesapeake Bay. The residual (observed minus modeled) salinity exhibits statistically significant linear ($p < 0.05$) trends between 1949 and 2006 in 13 of the 23 segments of the bay. The salinity change estimated from the trend line over this period varies from −2.0 to 2.2, with 10 of the 13 cells showing positive changes. The mean and median salinity changes over all 23 cells are 0.47 and 0.72; over the 13 cells with significant trends they are 0.71 and 1.1. We ran a hydrodynamic model of the bay under present-day and reduced sea level conditions and found a bay-average salinity increase of about 0.5, which supports the hypothesis that the salinity residual trends have a significant component due to sea-level rise. Uncertainties remain, however, due to the spatial and temporal extent of historical salinity data and the infilling of the bay due to sedimentation. The salinity residuals also exhibit interannual variability, with peaks occurring at intervals of roughly 7 to 9 years, which are partially explained by Atlantic Shelf salinity, Potomac River flow and the meridional component of wind stress.

Citation: Hilton, T. W., R. G. Najjar, L. Zhong, and M. Li (2008), Is there a signal of sea-level rise in Chesapeake Bay salinity?, *J. Geophys. Res.*, *113*, C09002, doi:10.1029/2007JC004247.

1. Introduction

[2] Global sea level has risen at a rate of approximately 1.7 ± 0.5 mm yr^{-1} during the second half of the 20th century [*Cabanes et al.*, 2001; *Church et al.*, 2004; *Bindoff et al.*, 2007] and is expected to increase at a substantially greater rate during the 21st century [*Bindoff et al.*, 2007]. One of the greatest expected impacts of sea-level rise is the intrusion of salt water into estuaries and groundwater [*McLean et al.*, 2001]. Because many species have a limited tolerance for salinity change, a long-term salinity increase may irreversibly damage estuarine ecosystems. *Kennedy et al.* [2002] argued that increases in sea level may act synergistically with other impacts on estuaries, such as climate-induced changes in streamflow and human development. For example, increased runoff in concert with sea-level rise could "squeeze" ecosystems by shrinking estuarine habitat. Similarly, sea-level rise may force ecosystems to move up the estuary, but development and pollution impacts at the head of the estuary may limit this migration. Rising salinity may also contaminate water supplies for drinking and industry, jeopardizing the livelihood of coastal communities. The importance of the problem is highlighted by current salinity management practices in a number of estuaries. For example, The Delaware River Basin Commission regularly releases water from reservoirs during periods of low streamflow in order to maintain salinity in Delaware Bay at acceptably low levels [*Hull et al.*, 1986].

[3] Despite the potentially large impacts of saltwater intrusion, we are aware of only one study that has attempted to estimate estuarine salinity trends due to sea-level rise from observations. *Wiseman et al.* [1990] analyzed several decades of salinity records in many Louisiana estuaries and found both positive and negative long-term trends, which were attributed to streamflow variability associated with local climate change.

[4] Numerical modeling studies support the contention that increases in sea level will increase estuarine salinity. Using a one-dimensional model of Delaware Bay, *Hull and Tortoriello* [1979] (also see *Hull and Titus* [1986]) estimated that a sea-level rise of 0.13 m would result in a chloride increase of 210 mg l^{-1} (a salinity increase of 0.4) in the upper portion of the estuary during low-flow periods (S ∼ 10). A one-dimensional model was also used by *Grabemann et al.* [2001] to simulate a 2-km upstream advance of the brackish water zone in the ∼80-km long Weser Estuary (Germany) for a sea-level rise of 0.55 m.

[5] The analysis of data collected from laboratory tests and prototype estuaries of constant cross-sectional area, as well as an analytical model of estuarine salt intrusion [*Savenije*, 1993], suggests the following relationship:

$$L \propto h_0 N^{-a} F^{-b}, \tag{1}$$

where L is the salt intrusion length (distance between estuary mouth and where the salinity is equal to the riverine

[1]Department of Meteorology, Pennsylvania State University, University Park, Pennsylvania, USA.
[2]Horn Point Laboratory, University of Maryland Center for Environmental Science, Cambridge, Maryland, USA.

Copyright 2008 by the American Geophysical Union.
0148-0227/08/2007JC004247

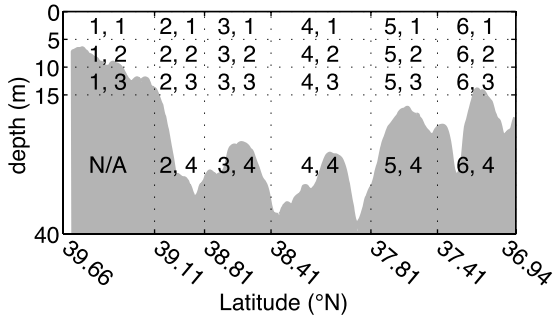

Figure 1. Model gridding scheme and maximum bay depth (gray).

salinity), h_o is the mean depth at the mouth of the estuary, N is Canter Cremer's estuary number, and F is the Froude number. Noting that F and N are inversely proportional to h_0 and using $a + b = 1$ [*Savenije*, 1993], we find that $L \propto h_0^2$. Thus, for example, if sea-level rise results in a 5% increase in h_0, L would be expected to increase by 10%.

[6] The present study considers the potential impact of sea-level rise on salinity in the Chesapeake Bay, a large and productive estuary in the Eastern United States. We chose the Chesapeake Bay due to its extensive salinity database and because relative sea-level rise there during the past 50 years is large (2.7 to 4.5 mm yr^{-1}, $n = 6$ [*Zervas*, 2001]) compared to the global average. This is due to land subsidence [*Nerem et al.*, 1998] as well as the greater rate of absolute sea-level rise in the middle latitudes of the Northwest Atlantic Ocean [*Church et al.*, 2004]. Chesapeake Bay is also an attractive choice for studying the influence of sea-level rise on estuarine salinity due to the availability of robust models of salinity in the bay, both statistical [*Gibson and Najjar*, 2000] and hydrodynamic (Regional Ocean Modeling System [ROMS] [*Li et al.*, 2005, 2006, 2007; *Zhong and Li*, 2006]).

[7] We hypothesize that sea-level rise has acted to increase Chesapeake Bay salinity, and we evaluate this hypothesis in two independent ways. First, we use the statistical salinity model of *Gibson and Najjar* [2000] to remove riverine influences and analyze long-term trends in the residual. Second, we conduct simulations of the response of Chesapeake Bay salinity to an increase in sea level using ROMS, a three-dimensional hydrodynamic model.

2. Methods

2.1. Statistical Salinity Model

[8] A statistical model was used to simulate Chesapeake Bay salinity for the 57-year period from 1949 to 2006 based on Susquehanna River flow, the single largest source of freshwater to the bay [*Schubel and Pritchard*, 1986] and the only river to discharge directly into the main stem bay. The model uses multiple linear regression to treat Chesapeake Bay salinity as a function of Susquehanna discharge. *Gibson and Najjar* [2000] demonstrated this type of model to be robust, capturing up to 93% of the variance in Chesapeake Bay salinity. Treating Bay salinity as a function only of streamflow means that the model residuals (observed salinity minus modeled salinity) contain the combined effects of other influences on estuarine salinity. Thus the residual trends over time quantify the long-term impacts on bay salinity of players such as rising sea level.

2.1.1. Model Domain and Grid

[9] As in *Gibson and Najjar* [2000], the bay was divided into six segments by latitude and four segments by depth (Figures 1 and 2). The boundaries of the latitude segments were chosen by *Harding and Perry* [1997] to divide the bay into characteristic salinity regimes. Because the northernmost segment is shallower than the rest of the bay there are only three depth segments in this column rather than four, resulting in a total of 23 cells over the entire bay. Hereafter, the grid cells are referenced by pairs of indices, with the first index specifying the north-to-south dimension and the second index specifying the surface-to-bottom dimension of the grid scheme, with indices increasing from north to south and from surface to bottom (Figure 1). The temporal resolution of the statistical model is monthly. Observed streamflow, discussed next, was used to force and calibrate the model.

2.1.2. Observed Data

[10] The statistical model for each of the 23 grid cells was forced by observed Susquehanna River discharge, and fit

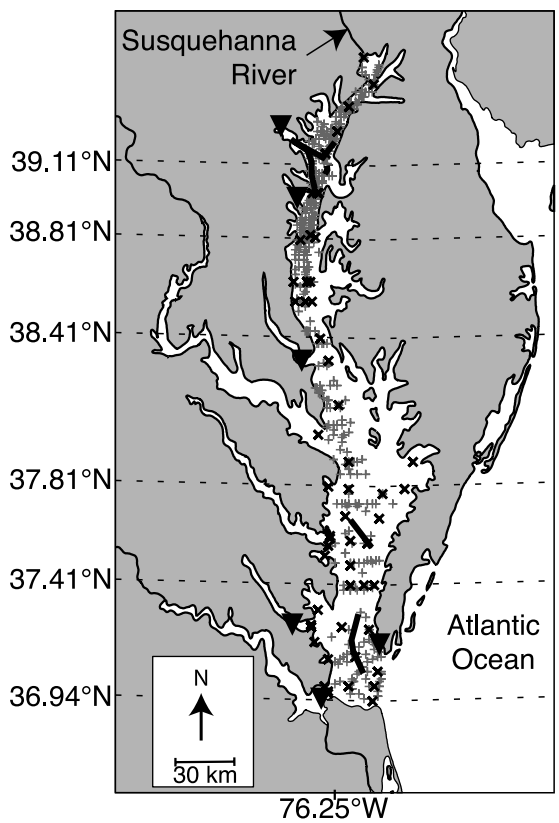

Figure 2. Locations of observations (symbols) and horizontal statistical model grid boundaries (dashed lines). 'X' markers denote CBP salinity measurements (1984–2006), crosses denote CBI salinity measurements (1949–1982), solid triangles show tide gauge stations from north to south: Baltimore, MD (station 8574680), Annapolis, MD (8575512), Solomons Island, MD (8577330), Gloucester Point, VA (8637624), Kiptopeke, VA (8632200), and Sewells Point, VA (8638610). Heavy black lines indicate (from North to South) Baltimore Harbor area channels, Rappahannock Shoal Channel, and York Spit Channel.

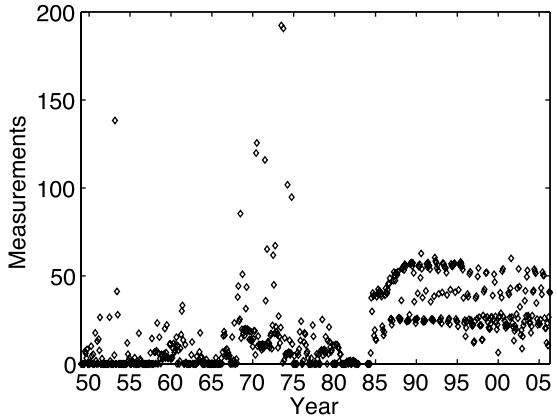

Figure 3. Mean number of salinity measurements per grid cell per month, 1949–2006. Horizontal axis labels correspond to January.

within each grid cell to observed salinity for 1984 to 2006. These observations are described below.

[11] The United States Geological Survey (USGS) provides Susquehanna River flow data, recorded at Conowingo, Maryland (USGS station 01578310) from October of 1967 through August of 2006, and at Harrisburg, Pennsylvania (USGS station 01570500), prior to 1967. Conowingo is approximately 15 km upriver from the mouth of the Susquehanna, while Harrisburg is approximately 100 km upriver from Conowingo [*Najjar*, 1999]. Using the conclusion of *Najjar* [1999], the Harrisburg flow was multiplied by 1.145 to estimate the Conowingo flow.

[12] Salinity data come from two sources: the Chesapeake Bay Program (CBP) and the Johns Hopkins Chesapeake Bay Institute (CBI). Both data sets were obtained from the CBP web site (www.chesapeakebay.net). The CBP is a joint venture of the U.S. Environmental Protection Agency, the Chesapeake Bay Commission, the District of Columbia, and the states of Maryland, Pennsylvania, and Virginia. The CBP provides approximately monthly salinity observations beginning in July 1984 and continuing through the present, averaging over 900 main stem salinity measurements per month. The CBI data span 1949 to 1982 and contain 230 main stem measurements per month on average. Many observations are clustered around a few particularly intense periods of several weeks, leaving many gaps of months or even years with no observations in some sections of the bay. The CBP and CBI data sets cover both the main stem bay and some of the larger tributaries. This study uses the main stem bay observations beginning in 1949 and ending in summer 2006, the most recent data that were available at the conclusion of the study. Both data sets provide good spatial coverage of the main stem bay, as shown in Figure 2. Figure 3 shows the mean number of observations recorded across all model grid cells each month since 1950, illustrating the temporal distribution of salinity measurements. Each individual grid cell shows a pattern similar to the mean pattern shown. The number of observations recorded per month rises sharply and becomes much more consistent with the beginning of the CBP record in July 1984.

2.1.3. Model Fitting

[13] The statistical salinity model is a linear regression of observed Chesapeake Bay salinity against observed Susquehanna River flow volume and thus treats salinity in the bay as a function solely of Susquehanna River discharge. Regression coefficients for each grid cell were determined using the observed monthly mean Susquehanna River flow rate for July 1984 through June 2006. Grid-cell mean salinity was calculated as the arithmetic mean of every observation made in the grid cell within each month. For each of the 23 grid cells, observed salinities were regressed against the river discharge of the current month and the previous five monthly river discharges. That is, in each grid cell the observed salinity for month m was regressed against the observed streamflows for months m, $m - 1$, …, $m - 5$. A set of coefficients was thus obtained to predict Chesapeake Bay salinity as a function of streamflow, resulting in the predictive equation:

$$S_m = \beta_0 F_m + \beta_1 F_{m-1} + \ldots + \beta_5 F_{m-5} + k. \qquad (2)$$

In this equation, S_m is the model salinity for month m, F_m is the observed Susquehanna discharge for month m, β_n is the regression coefficient for Susquehanna River flow at month $m - n$, and k is a constant. The model predicts the current salinity based on conditions during the prior 6 months, which is adequate because the mean ocean–bay exchange time is approximately 90 days [*Austin*, 2002].

[14] A second model structure including the previous 6 months of observed salinities was also considered to reflect the influence of previous salinity conditions on present salinity [*Gibson and Najjar*, 2000]. These additional salinity terms were analogous in structure to the flow terms in equation (2), and considered the salinities for months $m - 1$, …, $m - 6$. Results from this model were nearly identical to the results from equation (2). Perhaps this should not surprise; unlike previous salinity conditions, which are merely descriptive, streamflow is a physical forcing agent for estuarine salinity. The more parsimonious model of equation (2) was thus adopted for the study.

2.1.4. Modeled Salinity and Salinity Residual

[15] Fifty-seven years of monthly salinity values were computed in each grid cell by applying the model coefficients to the current and the previous 5 months of observed river flow. The model results reconstruct the historical variations in Chesapeake Bay salinity caused by

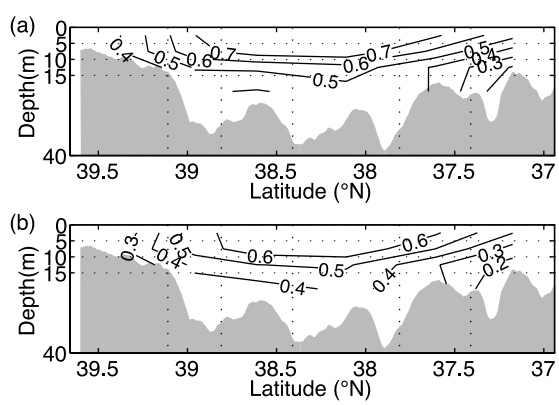

Figure 4. Model r^2 value contours, with maximum bay depth in gray. Grid scheme corresponds to Figure 1. (a) Full model, (b) anomaly model.

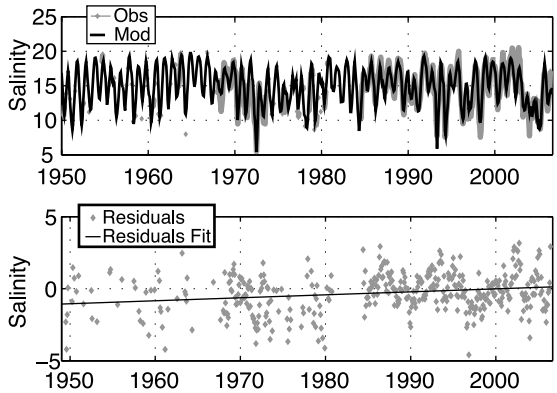

Figure 5. Salinity and residual time series for cell (4, 1). Model $r^2 = 0.78$.

streamflow only. Figure 4a contours the model skill in recreating bay salinities, as measured by the r^2 for the model output versus observed salinities for 1949 to 2006. The results are similar to those found by *Gibson and Najjar* [2000], with r^2 values for the shallower depths in the mid-bay Region being the highest and with four cells showing $r^2 > 0.75$. The low skill near the mouth of the Susquehanna River may be due to short-term fluctuations in streamflow and salinity that are not captured by the observed sampling frequency and the statistical model [*Gibson and Najjar*, 2000]. To determine salinity variability due to processes other than streamflow, we computed the salinity residual, which is the observed salinity minus the salinity predicted by the statistical model. We determined long-term trends in the residual using least-squares linear fits.

2.1.5. The Anomaly Model

[16] Salinity in the Chesapeake Bay is subject to a strong annual cycle that lags streamflow by several weeks. Susquehanna River flow typically peaks in April and reaches its minimum in August, and bay salinity typically reaches an annual minimum in May and an annual maximum in October or November. Model skill as measured by r^2 is certainly, to some extent, a reflection of the ability to capture the annual cycle. Forces that impact salinity only over many years have a smaller influence on the overall salinity than does the annual cycle. Therefore the model could conceivably perform quite poorly with respect to longer timescales and still achieve a skillful r^2 on account of the annual cycle alone.

[17] Due to our interest in processes affecting salinity at the timescale of decades, we also constructed a statistical model in which the annual cycle is removed. In this model, the observed Susquehanna discharge values are replaced by observed Susquehanna flow anomalies, where the anomaly is defined by the value for a given month minus the mean value for that month over the period 1984 to 2006. A set of anomaly coefficients, analogous to β_n in equation (2), was generated using least-squares multiple linear regression with the same number of lags as in the full salinity model. Figure 4b shows the skill of this model calculated for 1949 to 2006. The r^2 pattern is similar to that of the full salinity model. The residual (observed minus modeled) anomaly was analyzed in the same way as the salinity residual from the full model.

2.2. Hydrodynamic Model

[18] The statistical salinity model described above provides diagnostic capability based on the observed behavior of the bay, but does not consider the physics that govern estuarine salinity. A hydrodynamic model, in contrast, is based on the governing equations of fluid mechanics and thus offers a point of view entirely independent from the statistical model presented in previous sections.

[19] We ran a configuration of the Regional Ocean Modeling System (ROMS) for the Chesapeake Bay [*Li et al.*, 2005]. The model has an orthogonal curvilinear coordinate system designed to follow the coastlines of the main stem. The grid spacing is less than 1 km in the cross-channel direction and about 2 to 3 km in the along-channel direction. The total number of horizontal grid points is 120 × 80 and there are 20 layers in the vertical direction. The model is forced by sea level at the open ocean boundary, freshwater inflows at river mouths, and wind stress and heat exchange across the water surface. Hindcast simulations were conducted for 2 years (1 January 1996 to 31 December 1997) with markedly different annual river discharges [*Li et al.*, 2005]. The model shows considerable skill in reproducing the observed temporal and spatial variability in salinity. Here we repeat the 2-year simulations of *Li et al.* [2005], but with the sea level reduced by 20 cm, which is within the range (14 to 22 cm, $n = 6$ [*Zervas*, 2001]) of the sea-level change recorded during the second half of the 20th century. This model run is presumed to represent a hypothetic sea level at the bay's mouth if the sea level did not rise over the past 50 years. Other boundary conditions (meteorological and hydrological) and the initial conditions are identical to the original simulations. To evaluate the impact of sea-level rise on salinity in the model, we simply examine the salinity differences between the model run forced at the lower sea level and the run forced at the current sea level.

3. Results

3.1. Statistical Model

[20] Figure 5 shows the observed salinity, model salinity, model residuals, and model residual trend for cell (4, 1), which is between 0 and 5 m depth and approximately halfway along the main stem bay (see Figure 1). The model performs well in cell (4, 1), where the r^2 value is 0.78. Table 1 presents an estimate of the change in the salinity residual for each cell over the 57-year period, computed simply as the slope of the linear fit to the residual time series multiplied by 57 years. The changes vary from −2.0 to 2.2, but 18 of the 23 grid cells show a positive change. The arithmetic-mean salinity change among all the cells is 0.47 and the median is 0.72.

[21] The p-value of a linear fit quantifies the probability that the true linear regression coefficients are all zero, that is,

Table 1. Total 1949–2006 Residual Salinity Changes Computed From Statistical Model Trends[a]

	North					South
0–5 m	−1.65	**1.99**	**1.20**	**1.18**	**1.85**	−2.04
5–10 m	−0.27	**0.75**	**0.85**	**0.40**	**2.19**	−1.68
10–15 m	**0.06**	**0.96**	**0.99**	**0.44**	**2.06**	**0.18**
>15 m		**1.09**	**1.08**	**0.07**	**0.45**	−0.19

[a]Values are slopes of the linear fit multiplied by 57 years. Boldface highlights salinity increases. Grid scheme corresponds to Figure 1.

Table 2. Model Residual Trend p-Values, 57-Year Run[a]

	North					South
0–5 m	$\mathbf{7.1 \cdot 10^{-5}}$	$\mathbf{2.2 \cdot 10^{-5}}$	$\mathbf{1.2 \cdot 10^{-2}}$	$\mathbf{9.2 \cdot 10^{-3}}$	$\mathbf{1.7 \cdot 10^{-3}}$	$\mathbf{1.8 \cdot 10^{-4}}$
5–10 m	$6.4 \cdot 10^{-1}$	$8.4 \cdot 10^{-2}$	$8.5 \cdot 10^{-2}$	$3.7 \cdot 10^{-1}$	$\mathbf{3.3 \cdot 10^{-4}}$	$\mathbf{1.3 \cdot 10^{-4}}$
10–15 m	$9.4 \cdot 10^{-1}$	$\mathbf{1.9 \cdot 10^{-2}}$	$\mathbf{3.7 \cdot 10^{-2}}$	$3.5 \cdot 10^{-1}$	$\mathbf{3.9 \cdot 10^{-4}}$	$6.2 \cdot 10^{-1}$
>15 m		$\mathbf{9.0 \cdot 10^{-3}}$	$\mathbf{1.3 \cdot 10^{-2}}$	$8.8 \cdot 10^{-1}$	$2.8 \cdot 10^{-1}$	$7.1 \cdot 10^{-1}$

[a]Boldface highlights significant p-values (≤ 0.05). Grid scheme corresponds to Figure 1.

that the calculated linear fit is a mere coincidence of the points sampled and no linear relation actually exists between the variables in question. Thus, a small p-value indicates that the slope of the linear fit is, to a high probability, an accurate measure of the true trend in the model residuals. p-values are discussed in many statistics texts [e.g., *Devore*, 1995].

[22] A standard p-value calculation for determining the significance of a linear trend uses a standard t-test, which assumes that the sample population consists of independent elements. There appears to be some periodicity to our model residuals, however: the residuals in Figure 5 show a period of roughly 7 to 9 years, with peaks near 2002, 1993, and 1986. This behavior was widespread among the 23 model grid cells, particularly between 1984 and 2006 when salinity observations were regular and extensive. This periodicity, discussed more extensively in section 4.4, indicates that the bay retains some memory of previous salinities. For the purposes of evaluating the statistical significance of model residual trends it is necessary to eliminate the influence of correlation within the residual series by determining the number of truly independent samples within the complete residual series of 684 months from 1949 to 2006.

[23] The effective sample size of uncorrelated elements within a series with first-order autocorrelation is approximated by the following equation given by *Wilks* [1995]:

$$n' \approx n \frac{1 - \rho_1}{1 + \rho_1}. \tag{3}$$

Here n' denotes the effective sample size, n the actual sample size (in this case, 684 months), and ρ_1 is the lag-1 autocorrelation coefficient. Autocorrelation and calculation of autocorrelation coefficients are discussed in many introductory statistics texts [e.g., *Wilks*, 1995]. n' varies from 24% to 73% of n (median = 44%) among the 23 cells.

[24] Table 2 presents the p-values for the linear fits to the residual time series, calculated using the effective sample size in each grid cell. In 13 of the 23 cells the p-value is less than 0.05. If we restrict our estimates of the mean and median salinity change over the 57-year period to these cells, we get 0.71 and 1.09, respectively. If we restrict our estimates of the mean and median salinity change over the 57-year period to the four cells that have p-values less than 0.05 and model r^2 (Figure 4a) greater than 0.6, we get 1.56 and 1.53, respectively.

[25] Our confidence in the residual trends would be reduced if we were forced to conclude that a study performed without the most recent few years of streamflow and salinity observations would reach a different conclusion. Figure 6 examines the marginal impact on the p-value of each additional month of data past July 1984. The leftmost point, at 1984 on the horizontal axis, shows the p-value for the linear fit of model residuals from 1949 through July of 1984; the 12th point from the left shows the p-value when residuals from 1949 through July of 1985 are used to calculate the trend; and the rightmost point, at 2006 on the horizontal axis, shows the p-value for the trend of all residuals, 1949 through August 2006. Thus the rightmost p-value in each grid cell is equal to the value reported in Table 2. The plots in Figure 6 show the p-values that would have resulted had the same experiment

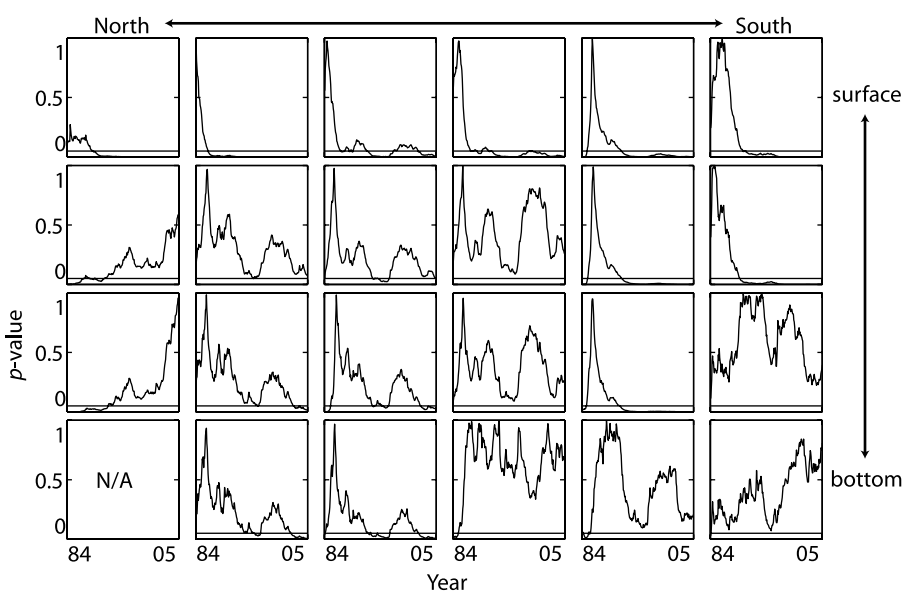

Figure 6. p-value (vertical axis) vs. months past July 1984 (horizontal axis). A horizontal line is drawn at $p = 0.05$. Grid scheme corresponds to Figure 1.

Table 3. Total 1949–2006 Salinity Changes Computed From Anomaly Model Trends[a]

	North					South
0–5 m	−1.58	**1.98**	**1.32**	**1.07**	**1.71**	−2.17
5–10 m	−0.23	**0.80**	**0.98**	**0.33**	**2.05**	−1.83
10–15 m	**0.00**	**0.98**	**0.98**	**0.27**	**1.89**	**0.08**
>15 m		**1.07**	**1.06**	−0.04	**0.29**	−0.28

[a]Values are slopes of the linear fit multiplied by 57 years. Boldface highlights salinity increases. Grid scheme corresponds to Figure 1.

been performed in the past, without the benefit of some portion of the salinity observations of the past 20 years. Many of the cells report fluctuating *p*-values right up to the present, which appear to respond to the interannual variations in model residuals (discussed more thoroughly in section 4.4). Eight cells show *p*-values that stabilize at significant levels by the early 1990s. If we restrict our estimates of mean and median salinity change over the past 57 year to those eight cells, we get values of 0.49 and 1.52, respectively. Further restricting to those cells with model $r^2 > 0.6$ leaves us with three cells, whose mean is 1.67 and median is 1.85.

[26] A final test of the significance of the trends in residual salinity is their sensitivity to whether or not the annual cycle is included in the model. Tables 3 and 4 show the residual salinity changes over the 57-year period and *p*-values for the anomaly model residuals, and are analogous to Tables 1 and 2. The slopes and *p*-values are similar for the full salinity model and the anomaly model. Thus, our conclusions about long-term trends in salinity, after removing streamflow effects, is independent of whether or not the annual cycle is included. This is because the full salinity model is nearly as effective at simulating the observed anomaly time series as the anomaly model (not shown), suggesting that a given streamflow change will result in the same salinity change regardless of whether it occurs over timescales of months or years.

[27] Overall, the statistical model results point toward increasing salinity in the Chesapeake Bay during the second half of the 20th century after removing the influence of streamflow, particularly when emphasis is given to those portions of the bay where model skill is relatively high and where residual slopes are significant. This result is independent of record length between about 45 and 57 years, and whether or not the annual cycle is included in the analysis.

3.2. Hydrodynamic Model

[28] Figure 7 shows a comparison of the salinity distribution along the center axis of the Chesapeake Bay between the present-day and reduced-sea-level simulations. To filter out short-term effects such as tides and winds, we averaged the salinity over 3 summer months (July–September 1997).

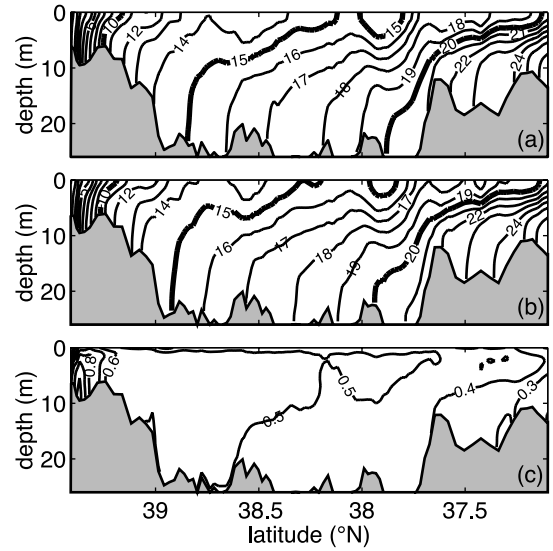

Figure 7. Along-channel distribution of salinity averaged over three summer months (July–September) of 1997: (a) model run forced at the current sea level; (b) model run forced at the reduced sea level; (c) salinity difference between the two model runs.

There are subtle but visible differences in the along-channel salinity distribution between the two model runs (compare Figures 7a and 7b). In particular, the 15 and 20 isohalines shift seaward in the model run with the reduced sea level. In other words, the sea-level rise causes saline water to intrude further landward as expected. In Figure 7c we plot the salinity difference between the two runs. It shows that the 20-cm sea-level rise causes salinity in the bay to increase by 0.3 to 0.8. The salinity increase is nearly uniform (0.5) in the middle part of the bay (37.5°–39.5° latitude). The salinity increase per unit of sea-level rise, about 0.025 cm^{-1}, is similar to 0.03 cm^{-1} in the upper portion of Delaware Bay that was estimated in the modeling study of *Hull and Tortoriello* [1979].

[29] The salinity distribution in the Chesapeake Bay not only depends on the shelf salinity and sea level but also on the amount of fresh water entering the bay. As shown in Figure 8a, the river runoff experiences large seasonal variations. This fresh-water forcing may affect the bay's response to sea-level rise. In Figure 8b we present the volume-averaged salinity over the whole bay. Indeed, the averaged salinity shows large seasonal variations in response to changes in the fresh water flow. For example, the large runoff in the winter (around day 25) of 1996 causes a rapid salinity reduction of 5. The series of high flows in the fall of 1996 and winter of 1997 (day 300–400) also cause significant drops in the mean salinity. In contrast, the

Table 4. Anomaly Model Residual Trend *p*-Values, 57-Year Run[a]

	North					South
0–5 m	$\mathbf{3.2 \cdot 10^{-3}}$	$\mathbf{1.5 \cdot 10^{-2}}$	$1.6 \cdot 10^{-1}$	$2.1 \cdot 10^{-1}$	$5.3 \cdot 10^{-2}$	$\mathbf{3.1 \cdot 10^{-3}}$
5–10 m	$7.5 \cdot 10^{-1}$	$2.7 \cdot 10^{-1}$	$2.6 \cdot 10^{-1}$	$6.7 \cdot 10^{-1}$	$\mathbf{7.9 \cdot 10^{-3}}$	$\mathbf{4.4 \cdot 10^{-4}}$
10–15 m	$10.0 \cdot 10^{-1}$	$6.4 \cdot 10^{-2}$	$6.5 \cdot 10^{-2}$	$6.4 \cdot 10^{-1}$	$\mathbf{4.6 \cdot 10^{-3}}$	$8.3 \cdot 10^{-1}$
>15 m		$\mathbf{2.6 \cdot 10^{-2}}$	$\mathbf{2.7 \cdot 10^{-2}}$	$9.4 \cdot 10^{-1}$	$5.4 \cdot 10^{-1}$	$6.0 \cdot 10^{-1}$

[a]Boldface highlights significant *p*-values ($\leq$0.05). Grid scheme corresponds to Figure 1.

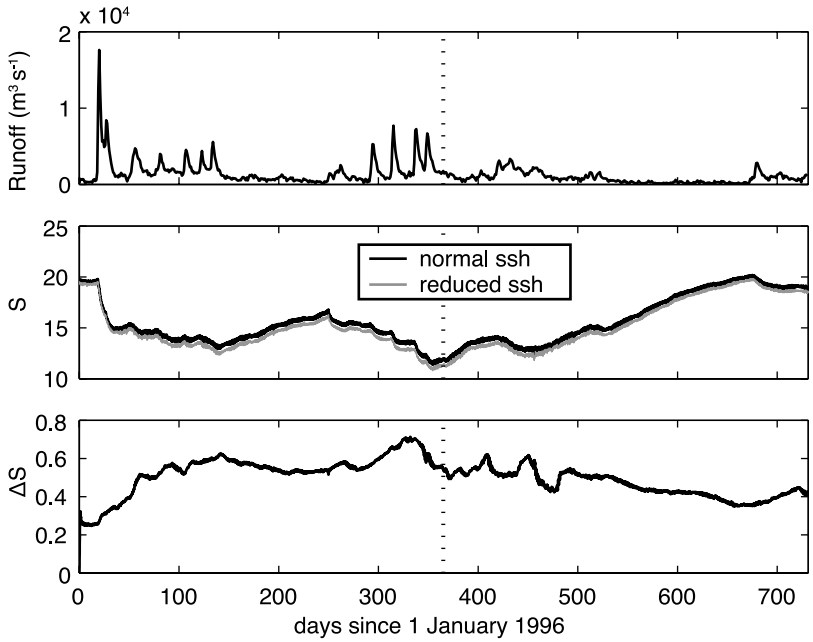

Figure 8. Time series of (a) Susquehanna River runoff, (b) bay-wide averaged salinity for the model run forced at the current sea level (black line) and the model run forced at the reduced sea level (gray line), and (c) bay-wide averaged salinity difference. The model integration begins on 1 January 1996 and ends on 31 December 1997.

salinity rebounds during dry summer periods. In particular, the mean salinity climbs by 8 during the dry period (day 450–780). Although both model runs show similar temporal variations, the run with the reduced sea level maintains a lower salinity throughout the 2 years. In Figure 8c we plot the time series of the mean salinity difference between the two model runs. In the beginning of the model integration, the sea-level drop at the open-boundary leads to a retreat of high-salinity water back to the shelf and a rapid drop in the mean salinity in the bay. This rapid response is similar to the rapid salinity increase that was observed in the lower bay during a storm surge [*Li et al.*, 2006]. The mean salinity difference appears to be a mirror image of the mean salinity, i.e., the salinity difference between the two model runs is higher when the mean salinity is lower. This suggests that Chesapeake Bay salinity may respond to sea-level rise more strongly during periods of high river runoff. This reflects a potential nonlinearity in the system, because salinity changes due to flow and sea-level rise are not simply additive but rather appear to be less than the sum of individual changes acting on the mean state.

4. Discussion

[30] When taken together, the similar main-stem-average salinity changes of ~0.5 over the second half of the 20th century found from the statistical and hydrodynamic approaches suggest that sea-level rise is having a detectable influence on Chesapeake Bay salinity. The salinity increase is also of the same magnitude that might be expected from the scaling of the salt intrusion length (L) with the mean depth at the mouth of the estuary (h_0). For the Chesapeake Bay, $h_0 \sim 10$ m [*Valle-Levinson et al.*, 1998]. For a 0.20-m rise in sea level, h_0 increases by roughly 2%, resulting in an increase of about 4% in L. Assuming that mean salinity in the bay (~15) scales linearly with L, we would expect a salinity increase of $0.04 \times 15 = 0.6$.

[31] However the results of each modeling exercise depend on assumptions that need to be examined further. Regarding the statistical model, we have assumed that data quality is sufficient to extract a long-term trend. However there may be substantial differences in quality between the CBI and CBP measurements, which have the potential to create a spurious long-term trend. With regard to the hydrodynamic model calculation, we have assumed no change in seafloor bathymetry. Such changes, however, may negate or enhance the effects of sea-level rise. For example, *Donoghue et al.* [1989] noted that sedimentation rates in the upper Chesapeake Bay are very close to rates of sea-level rise. On the other hand, dredging of navigation channels may have allowed more salt water to enter the bay. Finally, our conclusions are also weakened by the considerable interannual variability in the salinity residual, particularly if they remain unexplained. These issues are now addressed in more detail.

4.1. Quality of Historical Salinity Data

[32] Salinometers (based on conductivity) in the mid-1950s could make measurements with an accuracy of 0.003, two orders of magnitude smaller than the salinity changes estimated here; even the earlier titration methods, which had an accuracy of 0.02, were reasonably good [*Pickard and Emery*, 1990, p. 97]. The CBI was a leader in the technological advancement of observational instrumentation, and during this time period created and refined the first instrumentation capable of in situ conductivity measurement [*Esterson*, 1957]. It therefore seems reasonable to assume that the CBI salinity data (1949–1982) are

of adequate accuracy for this study. The CBP followed well-documented practices and used modern equipment and measurement techniques in collecting its salinity observations from 1984 to 2006 [*Chesapeake Bay Program*, 1993], and so we are also confident in the quality of the CBP salinity data set.

[33] The major difference between the CBI and CBP data set is temporal and spatial coverage. The CBI made observations at haphazard time intervals, particularly in its early years (Figure 3). This results in poor temporal resolution in the 1950s and early 1960s and a sparser picture of Chesapeake Bay salinity than that delivered by the CBP. Therefore, in spite of the technological achievements of the CBI, it is possible that the adoption of the CBP sampling strategy in 1984 introduced a discontinuity in the salinity series. Such a discontinuity could introduce a spurious linear trend into the statistical model residual series. To assess the contribution of the CBI data set to the calculated residual trends, we calculated linear trends for the model residuals from 1984 to 2006 only. If these modern-era residuals were to display trends similar to those observed over the entire 57-year period beginning in 1949, we could conclude that the positive slopes are not an artifact of the data collection practices. However no statistically significant trend exists in these modern residuals, as the regression p-values are between 0.40 and 0.99 in all but three model cells, and nowhere lower than 0.15. In summary, while we are confident in the CBI salinity observations, the more recent CBP data cannot independently confirm the salinity trends of the statistical model.

4.2. Sedimentation

[34] Land subsidence and absolute sea-level rise are not the only processes with the potential to alter the equilibrium between sea level and Chesapeake Bay salinity. Vast amounts of sediment enter the bay via rivers, shoreline erosion and the Atlantic Ocean, eventually settling to the bottom and accumulating on the bay's bed [*Cronin et al.*, 2003a]. Sedimentation is not detected by tide gauges but could mitigate the effects of relative sea-level rise by making the bay shallower. It has proven difficult to measure the rate of sedimentation precisely, owing to both the nature of the process as well as large spatial variability in accumulation. *Cronin et al.* [2003b] compiled the results of several different investigators that used different methods to measure sedimentation rates and concluded that sedimentation adds between 1 and 10 mm yr^{-1} to the bed of the bay. The uncertainty in this figure not only spans an order of magnitude, but could be significantly higher or lower than the roughly 3–4 mm yr^{-1} rise in relative sea level in the bay during the second half of the 20th century.

[35] The sedimentation rate varies significantly with location throughout the bay. By examining sediment core samples from around the bay, *Officer et al.* [1984] concluded that the rate is much higher in the northern and southern ends of the bay than in the central main stem bay because the Susquehanna River and the Atlantic Ocean are both large sources of suspended sediment. Estimating regional rates by fitting a least-squares curve to the core sedimentation rates versus latitude, *Officer et al.* [1984] report that sedimentation contributes 0.3 to 1.2 g cm^{-2} yr^{-1} in the north end of the bay, 0.1 to 0.3 g cm^{-2} yr^{-1} in the central region (roughly corresponding to latitude bins 2, 3, 4 and 5), and 0.1 to 0.8 g cm^{-2} yr^{-1} in the south. Using the dry bulk sediment density of 0.7 g cm^{-3} reported by *Donoghue et al.* [1989], these accumulations amount to 4–17 mm yr^{-1} in the north, 1–4 mm yr^{-1} in the mid-bay, and 1–11 mm yr^{-1} in the south. Interestingly, the regions of high sediment accumulation (latitude bins 1 and 6) are the only places where the statistical model estimates long-term salinity decreases. To summarize, sedimentation rates in the northern part of the bay equal or exceed the rate of sea-level rise, whereas in the remainder of the bay sedimentation rates range from several times smaller to several times greater than rates of sea-level rise.

4.3. Dredging

[36] While sedimentation mitigates impacts of sea-level rise on salinity, dredging has the potential to enhance them. Regular dredging of shipping channels through the central main stem bay is necessary to maintain shipping access to Baltimore Harbor. Because saltwater is more dense than freshwater and flows landward through an estuary at depth, the deep main stem channel provides the major conduit for saltwater to enter the bay. We acquired records from the U.S. Army Corps of Engineers to determine where and when the main stem Chesapeake Bay has been dredged. There have been three main sites of dredging along the axis of the main stem bay, as shown in Figure 2: York Spit Channel, Rappahannock Shoal Channel, and the Baltimore Harbor area, which contains the Craighill, Brewerton, Tolchester, and Swan Point Channels. Typical channel widths are 0.2 to 0.3 km (600 to 1000 ft), which can be compared with cross-channel distances that vary from about 10 to 40 km at the boundaries of the statistical model grid boxes.

[37] The York Spit Channel is roughly 29 km long, begins near the center of the bay's mouth, and hugs the axis of the main stem bay. It nearly bisects the southernmost grid segment of the statistical model, which is also the area in which *Officer et al.* [1984] report heavy sediment accumulation from the Atlantic Ocean. U.S. Army Corps of Engineers records indicate that the York Spit channel was dredged from 1961 to 1965, and in 1969, 1970, 1973, 1976, 1987, 1989, and 1994, with major deepening or widening taking place from 1961 to 1965, in 1969, and from 1987 to 1989. The Rappahannock Shoal Channel, 16 km in length, cuts through the mid-bay shallows for which it is named, beginning roughly 72 km north of the Atlantic Ocean and extending to the northwest. The Rappahannock Shoal Channel saw deepening work between 1961 and 1964, and again between 1987 and 1989. The Craighill and Brewerton Channels combine for 21.6 km and were dredged nearly every year from 1950 to present. The Tolchester Channel, 10.4 km long, was dredged at intervals of 3 to 5 years beginning in 1980.

[38] Thus, throughout most of the second half of the 20th century, the main stem bay has been continually and consistently dredged. Dredging frequencies do not appear to have changed in any obvious way throughout this time, but two of the channels were deepened during the 1960s and again during the late 1980s. It is possible that this deepening work impacted the salinity structure of the bay. It seems likely that a sudden, significant forcing would produce a

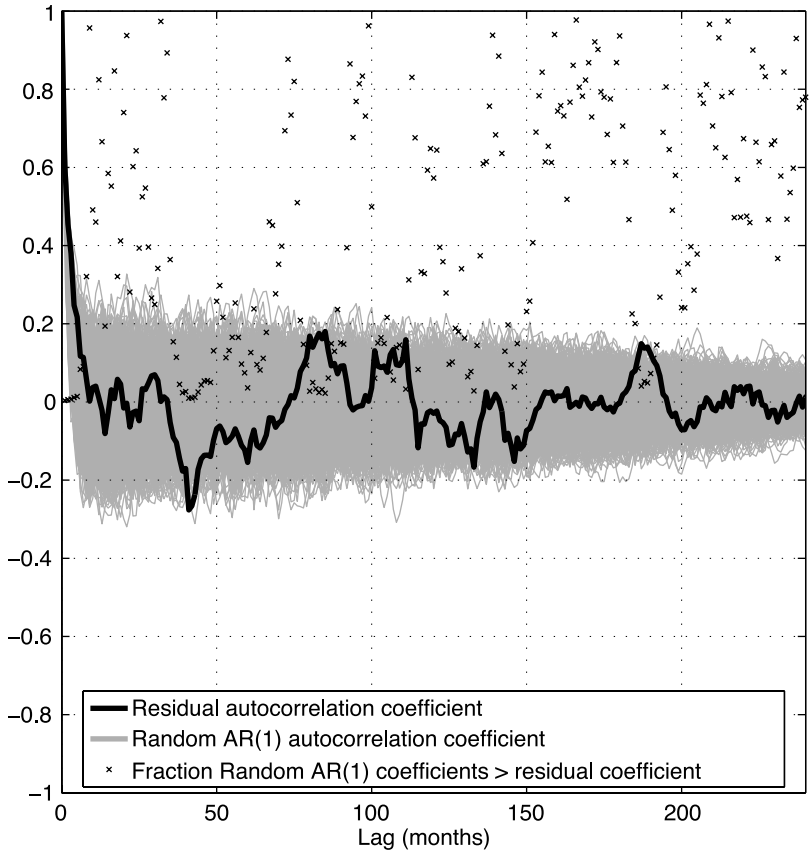

Figure 9. Autocorrelation coefficient vs. lag for model grid cell (4, 1) (black), 1000 AR(1) series drawn from normal distribution (gray). 'X' markers show the proportion of random AR(1) series with a higher autocorrelation coefficient than the residual series.

step-like discontinuity in the statistical salinity model residuals. Because no obvious step appears in the residual series, we suggest that dredging and deepening have had minimal impact on salinity change from 1950 to 2004. To investigate this further would require the use of hydrodynamic models that can explicitly resolve navigation channels [e.g., *U.S. Army Corps of Engineers*, 1997].

4.4. Residual Periodicity

[39] In section 3.1 we discussed the apparent periodicity in model residuals from the standpoint of evaluating the statistical significance of the residual trends but did not examine the periodic structure in its own right. As noted, the model residuals from grid cell (4, 1) shown in Figure 5 appear to exhibit a periodic tendency with peaks around 1986, 1993, and 2002, and similar structure appears in many of the model cells, particularly in latitude bins 2, 3, 4, and 5.

[40] The Chesapeake Bay salinity residual series is autocorrelated: the month following a month with an unusually high or low residual is likely to report an anomaly of the same sign. The residual will then eventually retreat back toward zero over some timescale. A random series with autocorrelation can appear to be periodic over short periods even though no true repeating structure exists [*Wunsch*, 1999]. A series that is truly periodic necessarily results in a maximum autocorrelation coefficient at lags equal to integral multiples of the period, because periodic signals by definition have similar values at intervals of one period. Thus a plot showing autocorrelation coefficient versus lag helps to understand whether any perceived periodicity is real.

[41] Figure 9 plots the autocorrelation coefficient against lag values for the model residuals from grid cell (4, 1), as well as for 1000 first-order autoregression, or AR(1), series drawn from a normal distribution. We analyze the autocorrelation from 1984 to 2003 only, because the scarcity of salinity observations prior to 1984 makes patterns difficult to discern. The residual autocorrelation coefficients reach a local maximum at lags between 80 and 100 months before decaying to zero, thereafter, and show strong negative autocorrelation at lags around 45 months. This indicates strong autocorrelation at periods of 7 to 9 years and fits with the observed peaks in the model residuals around 1986, 1993, and 2002.

[42] The residual autocorrelation coefficients are within the upper and lower bounds of the random series at all lags, which implies that a random AR(1) series is capable of producing the autocorrelation sequence produced by the residuals. Figure 9 also shows the proportion of the 1000 random AR(1) series that produce more extreme autocorrelation coefficients than the model residuals at any lag. These probabilities that a random series would report a higher autocorrelation coefficient than the residual series are essentially p-values for the autocorrelation coefficients. At lags of roughly 80 and 100 months, only a very small number of random series have higher autocorrelation coef-

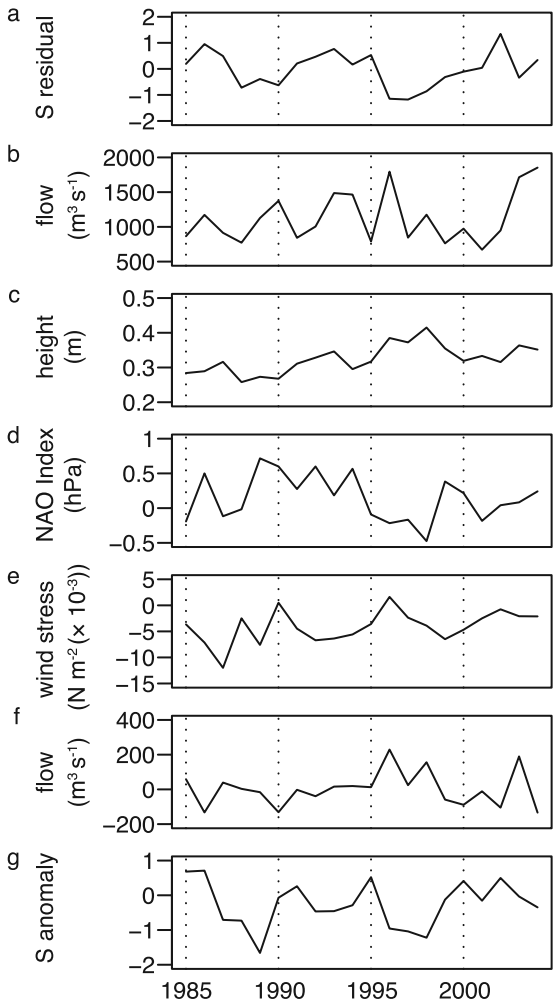

Figure 10. (a) Amplitude series for the first EOF of the annual mean salinity residual across the 23 cells for 1985 to 2004. The amplitudes are multiplied by the mean of the first EOF (0.20) to approximate the salinity residual magnitudes. (b) Annual mean Susquehanna River flow, m^3/s. (c) Annual mean of six Chesapeake Bay tide gauges, m. (d) Annual mean NAO index (hPa). (e) Annual mean meridional component of wind stress at Norfolk, VA, N m^{-2}. (f) Annual mean Potomac-Susquehanna residual, m^3/s. (g) Annual mean Atlantic Shelf salinity anomaly measured by Northeast Fisheries Science Center.

ficients than the residuals, and results are similar for most of the 16 grid cells in latitude bins 2, 3, 4, and 5 (not shown). Thus there is a real periodicity in model residuals.

[43] Though the periodicity of the model residuals is real, it could still be an artifact of the model. It appears that residuals tend to be high when salinity is high (e.g., the late 1980s, Figure 5), which is when streamflow is low. This may reflect the difficulty of statistical models in capturing extremes. To characterize the interannual variability of the residual time series from all grid cells across the bay, we compute empirical orthogonal functions (EOFs). The first EOF accounts for 80% of the variance in the model residuals. Figure 10a shows the first EOF amplitude series, which displays the same interannual variability seen in the residual time series of Figure 5. The amplitudes in Figure 10a are multiplied by the mean value of the first EOF (equal to 0.20) to put the magnitudes in the same range as the model residuals. Figure 10b shows annual averages of Susquehanna River flow. The correlation with the first EOF is very weak ($r = -0.20$), indicating that Susquehanna flow is not linearly related to the interannual variability in the residuals and ruling out poor model replication of extreme salinities as the cause of the residual periodicity.

[44] Having established the validity of the periodicity and ruled out model artifacts from extreme salinities as the cause, it is natural to entertain other possibilities. An obvious candidate is relative sea level itself, which is known to have significant decadal-scale variations in the Eastern United States, most likely due to wind-driven Rossby waves [*Hong et al.*, 2000]. To determine the relationship between relative sea levels and model residuals, we examine Chesapeake Bay tide gauge records. NOAA, through the National Ocean Service (NOS) Center for Operational Oceanographic Products and Services (COOPS), operates tide gauges at various locations around the Chesapeake Bay, several of which have continuous monthly records dating to the early 20th Century. We chose six of the 16 COOPS tide gauges in the Chesapeake Bay for their distribution in covering the main stem bay (Figure 2) and their relatively complete historical records. The annual records are highly correlated, with the correlation coefficient between station pairs varying from 0.81 to 0.99, with a median correlation of 0.93. Figure 10c shows the annual sea level in the Chesapeake Bay, based on an average of the six selected COOPS stations, revealing maxima around 1983, 1987, 1993, and 1998. The correlation coefficient between the first EOF and sea level is −0.33. This indicates that sea-level variations are an unlikely cause of the observed residual periodicity because the correlation coefficient has a small magnitude and a sign opposite to what is expected on physical grounds.

[45] Larger-scale climate forcing is another candidate cause of residual periodicity. Figure 10d shows the annual mean North Atlantic Oscillation (NAO) index [*NOAA Climate Prediction Center* [CPC]-a [2006a]], whose correlation coefficient with the first EOF is 0.26. The first EOF showed a correlation coefficient of 0.08 with the Niño3 index [*NOAA Climate Prediction Center* [CPC]-b [2006b]]. It would appear, then, that neither of these large-scale climate phenomena exerts a considerable influence on our residual variability.

[46] Regional wind patterns affect Chesapeake Bay salinity by affecting surface currents along the Atlantic shelf [*Wang*, 1979]. To measure this contribution, Figure 10e shows the annual mean of the meridional wind stress component. Wind stresses were calculated using the method of *Gill* [1982] with wind velocities recorded at Norfolk International Airport (WBAN station 13737). Norfolk, Virginia, is located near the mouth of the Chesapeake Bay. The wind data are available from NOAA's National Climatic Data Center (NCDC) as part of the hourly global surface data set (http://lwf.ncdc.noaa.gov/oa/climate/climatedata.html, data set 3505). Northerly winds drive eastward Ekman flow, forcing more salt water from the Atlantic Shelf into the bay. Regional winds appear to have some influence over the model residuals, with the correlation coefficient between the meridional wind stress component and the first EOF amplitude series equal to −0.40. Here, negative wind

stress values correspond to winds from the north. This correlation has the sign that one would expect from physical intuition, and indicates that local winds could account for up to 16% of the variability in the model residuals.

[47] The Susquehanna River is the bay's dominant tributary, but the Potomac River does contribute 16% of the riverine discharge to the bay. The flowrates of the two rivers are highly correlated [*Gibson and Najjar*, 2000], but any periodic oscillation in the uncorrelated portions could appear in the salinity model residuals, because the model considers only Susquehanna discharge. We remove from consideration the portion of Potomac River discharge that is correlated to the Susquehanna by modeling the Potomac discharge as a linear function of the Susquehanna discharge, then calculating residuals (defined as the observed Potomac discharge minus the modeled Potomac discharge). These annual mean Potomac-Susquehanna residuals are shown in Figure 10f, and the correlation coefficient with the first EOF amplitude series is −0.49. This has the expected sign, and the magnitude is such that almost 25% of the variability in salinity residual is explained by the Potomac residual flow.

[48] Any long-period variation in the Atlantic Shelf salinity near the mouth of the bay could certainly have a signal in Chesapeake Bay salinity. Between 1977 and 2004 the Northeast Fisheries Science Center (NEFSC) has measured salinity several times per year throughout the southern Mid-Atlantic Bight, from approximately 35.5° N to 40.5° N [*Mountain et al.*, 2004] The data set includes observed salinities as well as salinity anomalies, obtained by subtracting the annual cycle observed from 1977 to 1987. These data are available at http://www.nefsc.noaa.gov/nefsc/publications/crd/crd0408/crd0408.pdf. Figure 10g shows the NEFSC observed Atlantic Shelf salinity anomalies. A linear fit to the anomalies shows a slight decreasing trend in Shelf salinity from 1977 to 2004, which is opposite the salinity trend the present study observed within the bay. However the correlation coefficient with the first EOF amplitude series is 0.61, suggesting that Atlantic Shelf salinity variations explain around 35% of the statistical model salinity residual.

[49] In summary, only Potomac residual flow, regional meridional wind stresses, and Atlantic Shelf salinity anomalies show strong and physically reasonable correlation with the salinity residual. Multiple linear regression of these three against the first EOF amplitude series gives an r^2 of 0.61, indicating that together these factors account for approximately 60% of the variance in model residuals. Variations in dredging activity are another possible contributor but seem unlikely because the period of enhanced dredging in the lower bay (1987–1989) is not associated with elevated salinities.

5. Conclusions

[50] A statistical model was used to recreate the monthly salinity time series between 1949 and 2006 in 23 grid cells covering the main stem Chesapeake Bay. Model residuals, defined as the model salinities subtracted from the observed salinities, increased over the 57-year duration of the model run, implying that something other than Susquehanna River flow has acted to increase the salinity of the bay since 1949. Least-squares linear fits to the model residual time series indicate salinity increases on the order of 0.5 to 2.0 over much of the main stem bay.

[51] Model residuals through much of the central main stem bay also displayed significant periodicity of 7 to 9 years. Up to 60% of the variability in the first EOF of the of the salinity residual is explained by the combined influences of Atlantic Shelf salinity anomaly, local wind stress, and the portion of Potomac River discharge that is not correlated to Susquehanna River discharge. Several other factors affecting regional climate processes showed little correlation to the model residuals: Susquehanna River Flow, the North Atlantic Oscillation index, the Niño3 Index, and relative sea level itself.

[52] Two different ROMS simulations of Chesapeake Bay dynamics for the years 1996 and 1997 were conducted. One was forced entirely by current sea level, and the other was forced by sea level lowered by 20 cm to approximate sea levels in 1950, near the beginning of our statistical model run. The ROMS results averaged across July to September of 1997 show salinity increases between 0.3 and 0.8 throughout most of the main stem bay, with the mid-bay region seeing increases on the order of 0.5. These results are of the same sign and magnitude as the salinity changes resulting from the statistical model, supporting the hypothesis that sea-level rise is the cause of the increase in residual salinity.

[53] What are the implications for future salinity change in the Chesapeake Bay? Global sea-level is projected to increase from 9 to 88 cm [*Church et al.*, 2001] to 50 to 140 cm [*Rahmstorf*, 2007] by 2100 under a variety of greenhouse gas emissions scenarios. If we add a local component of sea-level rise of 0.9 to 2.7 mm yr^{-1} (or 9 to 27 cm over the 21st century) determined from the difference between global (1.8 mm yr^{-1}) and local (2.7 to 4.5 mm yr^{-1}) rates during the second half of the 20th century, we estimate a relative sea-level rise by 2100 of 18 to 167 cm in the Chesapeake Bay. Given a sensitivity of salinity to sea level of 0.02 to 0.07 cm^{-1}, we estimate a salinity change in the Chesapeake Bay of 0.4 to 12 by 2100. These can be compared with bay maximum salinity changes by 2100 of −0.25 to 2.0 due to climate-induced changes in streamflow [*Gibson and Najjar*, 2000].

[54] The potentially large future salinity change associated with sea-level rise would have disastrous effects for estuarine ecosystems and society. It is therefore important that further research be conducted to better quantify the relationship between sea level and salinity. Specifically it is important to better quantify changes in the bathymetry of the bay, both due to sedimentation and dredging, and to quantify those impacts on salinity through modeling. We also would encourage the application to other estuaries of the statistical and hydrodynamic modeling approaches developed here. Finally, a better understanding of interannual variability in estuarine and shelf salinity would be helpful to evaluate and calibrate models of long-term salinity change in estuaries.

[55] **Acknowledgments.** The authors thank William Boicourt, Mark Roulston, Klaus Keller, and two anonymous reviewers for helpful feedback on this research. Richard Klein provided dredging records from the U.S. Army Corps of Engineers, Norfolk District, and Jeffrey McKee provided dredging records from the USACE, Baltimore District. This work was supported by a National Science Foundation Small Grant for Exploratory

Research (OCE 0444005) and satisfied the Masters Thesis requirements of TWH. Any opinions, findings, and conclusions or recommendations expressed in this material are those of the authors and do not necessarily reflect the views of the National Science Foundation.

References

Austin, J. (2002), Estimating the mean ocean-bay exchange rate of the Chesapeake Bay, *J. Geophys. Res.*, *107*(C11), 3192, doi:10.1029/2001JC001246.

Bindoff, N., et al. (2007), Observations: Oceanic climate change and sea level, in *Climate Change 2007: The Physical Science Basis. Contribution of Working Group I to the Fourth Assessment Report of the Intergovernmental Panel on Climate Change*, edited by S. Solomon et al., chap. 5, Cambridge Univ. Press, New York.

Cabanes, C., A. Cazenave, and C. Le Provost (2001), Sea level rise during past 40 years determined from satellite and in situ observations, *Science*, *294*, 840–842.

Chesapeake Bay Program (1993), *Guide to Using the Chesapeake Bay Program Water Quality Monitoring Data*, 122 pp, Chesapeake Bay Program, Annapolis, MD.

Church, J., J. Gregory, P. Huybrechts, M. Kuhn, K. Lambeck, M. Nhuan, D. Qin, and P. Woodworth (2001), Changes in sea level, in *Climate Change 2001:The Scientific Basis. Contribution of Working Group I to the Third Assessment Report of the Intergovernmental Panel on Climate Change*, chap., p. 881, Cambridge Univ. Press, New York.

Church, J., N. White, R. Coleman, K. Lambeck, and J. Mitrovica (2004), Estimates of the regional distribution of sea level rise over the 1950–2000 period, *J. Clim.*, *17*, 2609–2625.

Cronin, T., S. Halka, and O. Bricker (2003a), Estuarine sediment sources, in *A Summary Report of Sediment Processes in Chesapeake Bay and Watershed: USGS Water-Resources Investigation Board Report 03-4123*, chap. 5, pp. 49–60, USGS.

Cronin, T., L. Sanford, M. Langland, D. Willard, and C. Saenger (2003b), Estuarine sediment, transport, deposition, and sedimentation, in *A Summary Report of Sediment Processes in Chesapeake Bay and Watershed: USGS Water-Resources Investigation Board Report 03-4123*, chap. 6, pp. 61–79, USGS.

Devore, J. (1995), *Probability and Statistics for Engineering and the Sciences*, 4th ed., Duxbury Press, Pacific Grove, Calif.

Donoghue, J., O. Bricker, and C. Olsen (1989), Particle-borne radionuclides as tracers for sediment in the Susquehanna River and Chesapeake Bay, *Estuarine Coastal Shelf Sci.*, *29*, 341–360.

Esterson, G. (1957), Induction conductivity indicator: A new method for conductivity measurements at sea, *Tech. Rep. 14*, 183 pp., Chesapeake Bay Institute.

Gibson, J., and R. Najjar (2000), The response of Chesapeake Bay salinity to climate-induced changes in streamflow, *Limnol. Oceanogr.*, *45*, 1764–1772.

Gill, A. (1982), *Atmosphere–Ocean Dynamics*, Academic Press, New York.

Grabemann, H., I. Grabemann, D. Herbers, and A. Muller (2001), Effects of a specific climate scenario on the hydrography and transport of conservative substances in the Weser estuary, Germany: A case study, *Clim. Res.*, *18*, 77–87.

Harding, L. J., and E. Perry (1997), Long-term increase of phytoplankton biomass in Chesapeake Bay, 1950–1994, *Mar. Ecol. Prog. Ser.*, *157*, 39–52.

Hong, B., W. Sturges, and A. Clarke (2000), Sea level on the U.S. east coast: Decadal variability caused by open ocean wind-curl forcing, *J. Phys. Oceanogr.*, *30*, 2088–2098.

Hull, C., and J. Titus (Eds.) (1986), *Greenhouse Effect, Sea Level Rise, and Salinity in the Delaware Estuary*, 88 pp., United States Environmental Protection Agency, Delaware River Basin Commission, Trenton, NJ.

Hull, C., and R. Tortoriello (1979), Sea-level trend and salinity in the Delaware Estuary, Staff Report, Delaware Basin Commission, West Trenton, NJ.

Hull, C., M. Thatcher, and R. Tortoriello (1986), *Greenhouse Effect, Sea Level Rise, and Salinity in the Delaware Estuary, chap. Salinity in the Delaware Estuary*, pp. 8–19, United States Environmental Protection Agency, Washington, D. C.

Kennedy, V., R. Twilley, J. Kleypas, J. Cowan, and S. Hare (2002), *Coastal and Marine Ecosystems and Global Climate Change: Potential Effects on U.S. Resources*, Pew Center on Global Climate Change, Arlington, VA.

Li, M., L. Zhong, and W. Boicourt (2005), Simulations of Chesapeake Bay estuary: Sensitivity to turbulence mixing parameterizations and comparison with observations, *J. Geophys. Res.*, *110*, C12004, doi:10.1029/2004JC002585.

Li, M., L. Zhong, W. Boicourt, S. Zhang, and D.-L. Zhang (2006), Hurricane-induced storm surges, currents and destratification in a semi-enclosed bay, *Geophys. Res. Lett.*, *33*, L02604, doi:10.1029/2005GL024992.

Li, M., L. Zhong, W. Boicourt, S. Zhang, and D.-L. Zhang (2007), Hurricane-induced destratification and restratification in a partially-mixed estuary, *J. Mar. Res.*, *65*, 169–192.

McLean, R., A. Tsyban, V. Burkett, J. Codignotto, D. Forbes, N. Mimura, and R. Beamish (2001), Coastal zones and marine ecosystems, in *Climate Change 2001: Impacts, Adaptation and Vulnerability*, chap., Cambridge Univ. Press, New York.

Mountain, D., M. Taylor, and C. Bascuñán (2004), *Revised procedures for calculating regional average water properties for Northeast Fisheries Science Center cruises*, Northeast Fish. Sci. Cent. Ref. Doc. 04-08, National Marine Fisheries Service, Woods Hole, MA.

Najjar, R. (1999), The water balance of the Susquehanna River and its response to climate change, *J. Hydrol.*, *219*, 7–19.

Nerem, R., T. van Dam, and M. Schenewerk (1998), Chesapeake Bay subsidence monitored as wetlands loss continues, *Eos Trans. AGU*, *79*.

NOAA Climate Prediction Center (CPC)-a (2006a), North Atlantic Oscillation. (Available at http://www.cpc.noaa.gov/products/precip/CWlink/pna/nao_index.html)

NOAA Climate Prediction Center (CPC)-b (2006b), Eastern Tropical Pacific SST (5N–5S, 150W–90W). (Available at http://www.cdc.noaa.gov/Correlation/nina3.data)

Officer, C., D. Lynch, G. Setlock, and G. Helz (1984), *The Estuary as a Filter*, pp. 131–157, chap. Recent Sedimentation Rates in Chesapeake Bay, p. 511, Academic Press, New York.

Pickard, G., and W. Emery (1990), *Descriptive Physical Oceanography: An Introduction*, 5th ed., 320 pp., Pergamon Press, New York.

Rahmstorf, S. (2007), A semi-empirical approach to projecting future sea-level rise, *Science*, 368–370.

Savenije, H. (1993), Predictive model for salt intrusion in estuaries, *J. Hydrol.*, *148*, 203–218.

Schubel, J., and D. Pritchard (1986), Responses of upper Chesapeake Bay to variations in discharge of the Susquehanna River, *Estuaries*, *9*, 236–249.

U.S. Army Corps of Engineers (1997), *Delaware River Main Channel Deepening Project, Supplemental Environmental Impact Statement*, chap. 5: Hydrodynamic Salinity Modeling, U. S. Army Corps of Engineers, Philadelphia District, North Atlantic Division.

Valle-Levinson, A., C. Li, T. Royer, and L. Atkinson (1998), Flow patterns at the Chesapeake Bay entrance, *Cont. Shelf Res.*, *18*, 1157–1177.

Wang, D.-P. (1979), Wind-driven circulation in the Chesapeake Bay, winter 1975, *J. Phys. Oceanogr.*, *9*, 564–572.

Wilks, D. (1995), *Statistical Methods in the Atmospheric Sciences: An Introduction*, Academic Press, New York.

Wiseman, W., E. Swenson, and J. Power (1990), Salinity trends in Louisiana estuaries, *Estuaries*, *13*.

Wunsch, C. (1999), The interpretation of short climate records, with comments on the North Atlantic and Southern Oscillations, *Bull. Am. Meteorol. Soc.*, *80*, 245–255.

Zervas, C. (2001), Sea level variations of the United States, 1854–1999, *Tech. Rep.*, NOAA, NOS CO-OPS 36.

Zhong, L., and M. Li (2006), Tidal energy fluxes and dissipation in the Chesapeake Bay, *Cont. Shelf Res.*, *26*, 752–770.

T. W. Hilton and R. G. Najjar, Department of Meteorology, Pennsylvania State University, 503 Walker Building, University Park, PA 16802, USA. (hilton@meteo.psu.edu)

M. Li and L. Zhong, Horn Point Laboratory, University of Maryland Center for Environmental Science, Cambridge, MD, USA.